Biomedical Optics EXPRESS

Raman difference spectroscopy: a non-invasive method for identification of oral squamous cell carcinoma

Christian Knipfer,[1,3,*] Johanna Motz,[1] Werner Adler,[4] Kathrin Brunner,[5] Medhaine Tesfay Gebrekidan,[2,3] Robert Hankel,[2,3] Abbas Agaimy,[5] Stefan Will,[2,3] Andreas Braeuer,[2,3] Friedrich Wilhelm Neukam,[1,3] and Florian Stelzle[1,3]

[1]*Department of Oral and Maxillofacial Surgery, Friedrich-Alexander Universität Erlangen-Nürnberg (FAU), Erlangen, Germany*
[2]*Lehrstuhl für Technische Thermodynamik, Friedrich-Alexander Universität Erlangen-Nürnberg (FAU), Erlangen, Germany*
[3]*Erlangen Graduate School in Advanced Optical Technologies (SAOT), Friedrich-Alexander Universität Erlangen-Nürnberg (FAU), Erlangen, Germany*
[4]*Department of Medical Informatics, Biometry and Epidemiology, Friedrich-Alexander Universität Erlangen-Nürnberg (FAU), Erlangen, Germany*
[5]*Department of Pathology, Friedrich-Alexander Universität Erlangen-Nürnberg (FAU), Erlangen, Germany*
**christian.knipfer@fau.de*

Abstract: The feasibility of shifted-excitation Raman difference spectroscopy (SERDS) as a label-free and non-invasive technique for an objective diagnosis of oral cancer (OSCC) was investigated by analyzing 12 *ex vivo* OSCC samples. 72 mean SERDS spectra from each three physiological tissue points and pathological lesions were correlated with the histo-pathological diagnosis. Principal component analysis (PCA) and linear discriminant analysis (LDA) showed excellent results with an area under the curve of 94.5% and a classification error of 9.7% (sensitivity: 86.1%; specificity: 94.4%). The SERDS Raman spectra of malignant and benignant tissues were discriminable with respect to the spectral features of proteins, lipids and nucleic acids. The presented method is capable of a highly accurate identification of OSCC. These findings suggest a high validity and reproducibility of SERDS combined with PCA and LDA analysis regarding oral cancer tissue.

OCIS codes: (170.0170) Medical optics and biotechnology; (170.5660) Raman spectroscopy; (170.6935) Tissue characterization; (170.3890) Medical optics instrumentation.

References and links

1. F. Berrino, G. Gatta; EUROCARE Working Group, "Variation in survival of patients with head and neck cancer in Europe by the site of origin of the tumours," Eur. J. Cancer **34**(14 14 Spec No), 2154–2161 (1998).
2. A. Forastiere, W. Koch, A. Trotti, and D. Sidransky, "Head and neck cancer," N. Engl. J. Med. **345**(26), 1890–1900 (2001).
3. E. E. Vokes, R. R. Weichselbaum, S. M. Lippman, and W. K. Hong, "Head and neck cancer," N. Engl. J. Med. **328**(3), 184–194 (1993).
4. M. W. Lingen, J. R. Kalmar, T. Karrison, and P. M. Speight, "Critical evaluation of diagnostic aids for the detection of oral cancer," Oral Oncol. **44**(1), 10–22 (2008).
5. P. Boyle and B. Levin, "World Cancer Report 2008," (World Health Organization, Lyon, 2008).
6. M. P. Coleman, G. Gatta, A. Verdecchia, J. Estève, M. Sant, H. Storm, C. Allemani, L. Ciccolallo, M. Santaquilani, and F. Berrino; EUROCARE Working Group, "EUROCARE-3 summary: cancer survival in Europe at the end of the 20th century," Ann. Oncol. **14**(5 Suppl 5), 128–149 (2003).
7. B. W. Neville and T. A. Day, "Oral cancer and precancerous lesions," CA Cancer J. Clin. **52**(4), 195–215 (2002).
8. J. Campo-Trapero, J. Cano-Sánchez, B. Palacios-Sánchez, J. J. Sánchez-Gutierrez, M. A. González-Moles, and A. Bascones-Martínez, "Update on molecular pathology in oral cancer and precancer," Anticancer Res. **28**(2B), 1197–1205 (2008).
9. S. Warnakulasuriya, J. Reibel, J. Bouquot, and E. Dabelsteen, "Oral epithelial dysplasia classification systems: predictive value, utility, weaknesses and scope for improvement," J. Oral Pathol. Med. **37**(3), 127–133 (2008).

#212874 - $15.00 USD Received 26 May 2014; revised 16 Jul 2014; accepted 31 Jul 2014; published 28 Aug 2014

10. A. Karabulut, J. Reibel, M. H. Therkildsen, F. Praetorius, H. W. Nielsen, and E. Dabelsteen, "Observer variability in the histologic assessment of oral premalignant lesions," J. Oral Pathol. Med. **24**(5), 198–200 (1995).
11. L. M. Abbey, G. E. Kaugars, J. C. Gunsolley, J. C. Burns, D. G. Page, J. A. Svirsky, E. Eisenberg, D. J. Krutchkoff, and M. Cushing, "Intraexaminer and interexaminer reliability in the diagnosis of oral epithelial dysplasia," Oral Surg. Oral Med. Oral Pathol. Oral Radiol. Endod. **80**(2), 188–191 (1995).
12. I. J. Bigio and S. G. Bown, "Spectroscopic sensing of cancer and cancer therapy: current status of translational research," Cancer Biol. Ther. **3**(3), 259–267 (2004).
13. H. Neumann, C. Langner, M. F. Neurath, and M. Vieth, "Confocal laser endomicroscopy for diagnosis of Barrett's esophagus," Front Oncol. **2**, 42 (2012).
14. M. A. Calin, S. V. Parasca, R. Savastru, M. R. Calin, and S. Dontu, "Optical techniques for the noninvasive diagnosis of skin cancer," J. Cancer Res. Clin. Oncol. **139**(7), 1083–1104 (2013).
15. J. K. Dhingra, D. F. Perrault, Jr., K. McMillan, E. E. Rebeiz, S. Kabani, R. Manoharan, I. Itzkan, M. S. Feld, and S. M. Shapshay, "Early diagnosis of upper aerodigestive tract cancer by autofluorescence," Arch. Otolaryngol. Head Neck Surg. **122**(11), 1181–1186 (1996).
16. A. Gillenwater, R. Jacob, R. Ganeshappa, B. Kemp, A. K. El-Naggar, J. L. Palmer, G. Clayman, M. F. Mitchell, and R. Richards-Kortum, "Noninvasive diagnosis of oral neoplasia based on fluorescence spectroscopy and native tissue autofluorescence," Arch. Otolaryngol. Head Neck Surg. **124**(11), 1251–1258 (1998).
17. R. J. Mallia, N. Subhash, A. Mathews, R. Kumar, S. S. Thomas, P. Sebastian, and J. Madhavan, "Clinical grading of oral mucosa by curve-fitting of corrected autofluorescence using diffuse reflectance spectra," Head Neck **32**(6), 763–779 (2010).
18. B. Swinson, W. Jerjes, M. El-Maaytah, P. Norris, and C. Hopper, "Optical techniques in diagnosis of head and neck malignancy," Oral Oncol. **42**(3), 221–228 (2006).
19. C. Krafft, B. Dietzek, and J. Popp, "Raman and CARS microspectroscopy of cells and tissues," Analyst (Lond.) **134**(6), 1046–1057 (2009).
20. R. Zhang, Y. Zhang, Z. C. Dong, S. Jiang, C. Zhang, L. G. Chen, L. Zhang, Y. Liao, J. Aizpurua, Y. Luo, J. L. Yang, and J. G. Hou, "Chemical mapping of a single molecule by plasmon-enhanced Raman scattering," Nature **498**(7452), 82–86 (2013).
21. M. Diem, P. R. Griffiths, and J. M. Chalmers, *Vibrational Spectroscopy for Medical Diagnosis* (John Wiley & Sons, Chichester, England, 2008).
22. S. Dochow, C. Krafft, U. Neugebauer, T. Bocklitz, T. Henkel, G. Mayer, J. Albert, and J. Popp, "Tumour cell identification by means of Raman spectroscopy in combination with optical traps and microfluidic environments," Lab Chip **11**(8), 1484–1490 (2011).
23. U. Neugebauer, T. Bocklitz, J. H. Clement, C. Krafft, and J. Popp, "Towards detection and identification of circulating tumour cells using Raman spectroscopy," Analyst (Lond.) **135**(12), 3178–3182 (2010).
24. K. Papamarkakis, B. Bird, J. M. Schubert, M. Miljković, R. Wein, K. Bedrossian, N. Laver, and M. Diem, "Cytopathology by optical methods: spectral cytopathology of the oral mucosa," Lab. Invest. **90**(4), 589–598 (2010).
25. R. J. Swain and M. M. Stevens, "Raman microspectroscopy for non-invasive biochemical analysis of single cells," Biochem. Soc. Trans. **35**(3), 544–549 (2007).
26. J. M. Schubert, B. Bird, K. Papamarkakis, M. Miljković, K. Bedrossian, N. Laver, and M. Diem, "Spectral cytopathology of cervical samples: detecting cellular abnormalities in cytologically normal cells," Lab. Invest. **90**(7), 1068–1077 (2010).
27. N. S. Eikje, K. Aizawa, and Y. Ozaki, "Vibrational spectroscopy for molecular characterisation and diagnosis of benign, premalignant and malignant skin tumours," Biotechnol. Annu. Rev. **11**, 191–225 (2005).
28. A. Nijssen, T. C. Bakker Schut, F. Heule, P. J. Caspers, D. P. Hayes, M. H. Neumann, and G. J. Puppels, "Discriminating basal cell carcinoma from its surrounding tissue by Raman spectroscopy," J. Invest. Dermatol. **119**(1), 64–69 (2002).
29. A. Robichaux-Viehoever, E. Kanter, H. Shappell, D. Billheimer, H. Jones 3rd, and A. Mahadevan-Jansen, "Characterization of Raman spectra measured in vivo for the detection of cervical dysplasia," Appl. Spectrosc. **61**(9), 986–993 (2007).
30. L. M. Almond, J. Hutchings, G. Lloyd, H. Barr, N. Shepherd, J. Day, O. Stevens, S. Sanders, M. Wadley, N. Stone, and C. Kendall, "Endoscopic Raman spectroscopy enables objective diagnosis of dysplasia in Barrett's esophagus," Gastrointest. Endosc. **79**(1), 37–45 (2014).
31. S. Luo, C. Chen, H. Mao, and S. Jin, "Discrimination of premalignant lesions and cancer tissues from normal gastric tissues using Raman spectroscopy," J. Biomed. Opt. **18**(6), 067004 (2013).
32. B. Brozek-Pluska, J. Jablonska-Gajewicz, R. Kordek, and H. Abramczyk, "Phase transitions in oleic acid and in human breast tissue as studied by Raman spectroscopy and Raman imaging," J. Med. Chem. **54**(9), 3386–3392 (2011).
33. A. S. Haka, K. E. Shafer-Peltier, M. Fitzmaurice, J. Crowe, R. R. Dasari, and M. S. Feld, "Diagnosing breast cancer by using Raman spectroscopy," Proc. Natl. Acad. Sci. U.S.A. **102**(35), 12371–12376 (2005).
34. H. Abramczyk, B. Brozek-Pluska, J. Surmacki, J. Jablonska-Gajewicz, and R. Kordek, "Raman 'optical biopsy' of human breast cancer," Prog. Biophys. Mol. Biol. **108**(1-2), 74–81 (2012).
35. A. T. Harris, A. Rennie, H. Waqar-Uddin, S. R. Wheatley, S. K. Ghosh, D. P. Martin-Hirsch, S. E. Fisher, A. S. High, J. Kirkham, and T. Upile, "Raman spectroscopy in head and neck cancer," Head Neck Oncol. **2**(1), 26 (2010).
36. N. Stone, P. Stavroulaki, C. Kendall, M. Birchall, and H. Barr, "Raman spectroscopy for early detection of laryngeal malignancy: preliminary results," Laryngoscope **110**(10), 1756–1763 (2000).

#212874 - $15.00 USD Received 26 May 2014; revised 16 Jul 2014; accepted 31 Jul 2014; published 28 Aug 2014

37. D. P. Lau, Z. Huang, H. Lui, C. S. Man, K. Berean, M. D. Morrison, and H. Zeng, "Raman spectroscopy for optical diagnosis in normal and cancerous tissue of the nasopharynx-preliminary findings," Lasers Surg. Med. **32**(3), 210–214 (2003).
38. D. P. Lau, Z. Huang, H. Lui, D. W. Anderson, K. Berean, M. D. Morrison, L. Shen, and H. Zeng, "Raman spectroscopy for optical diagnosis in the larynx: preliminary findings," Lasers Surg. Med. **37**(3), 192–200 (2005).
39. R. Malini, K. Venkatakrishna, J. Kurien, K. M. Pai, L. Rao, V. B. Kartha, and C. M. Krishna, "Discrimination of normal, inflammatory, premalignant, and malignant oral tissue: a Raman spectroscopy study," Biopolymers **81**(3), 179–193 (2006).
40. M. Diem, A. Mazur, K. Lenau, J. Schubert, B. Bird, M. Miljković, C. Krafft, and J. Popp, "Molecular pathology via IR and Raman spectral imaging," J. Biophotonics **6**(11-12), 855–886 (2013).
41. S. P. Singh, A. Deshmukh, P. Chaturvedi, and C. Murali Krishna, "In vivo Raman spectroscopic identification of premalignant lesions in oral buccal mucosa," J. Biomed. Opt. **17**(10), 1050021 (2012).
42. S. P. Singh, A. Sahu, A. Deshmukh, P. Chaturvedi, and C. M. Krishna, "In vivo Raman spectroscopy of oral buccal mucosa: a study on malignancy associated changes (MAC)/cancer field effects (CFE)," Analyst (Lond.) **138**(14), 4175–4182 (2013).
43. K. Guze, H. C. Pawluk, M. Short, H. Zeng, J. Lorch, C. Norris, and S. Sonis, "Pilot study: Raman spectroscopy in differentiating premalignant and malignant oral lesions from normal mucosa and benign lesions in humans," Head Neck ePub doi: 10.1002/hed.23629 (2014).
44. M. Yasser, R. Shaikh, M. K. Chilakapati, and T. Teni, "Raman spectroscopic study of radioresistant oral cancer sublines established by fractionated ionizing radiation," PLoS ONE **9**(5), e97777 (2014).
45. K. Venkatakrishna, J. Kurien, K. M. Pai, M. Valiathan, N. N. Kumar, C. Murali Krishna, G. Ullas, and V. Kartha, "Optical pathology of oral tissue: a Raman spectroscopy diagnostic method," Curr. Sci. **80**(5), 665–669 (2001).
46. A. P. Oliveira, R. A. Bitar, L. Silveira, Jr., R. A. Zângaro, and A. A. Martin, "Near-infrared Raman spectroscopy for oral carcinoma diagnosis," Photomed. Laser Surg. **24**(3), 348–353 (2006).
47. T. Hastie, R. Tibshirani, and J. Friedman, *The Elements of Statistical Learning* (Springer New York, 2001).
48. R Development Core Team, R: A language and environment for statistical computing. R Foundation for Statistical Computing, Vienna, (2008)
49. M. A. da Silva Martins, D. G. Ribeiro, E. A. Pereira Dos Santos, A. A. Martin, A. Fontes, and H. da Silva Martinho, "Shifted-excitation Raman difference spectroscopy for in vitro and in vivo biological samples analysis," Biomed. Opt. Express **1**(2), 617–626 (2010).
50. S. B. Cartaxo, I. D. Santos, R. Bitar, A. F. Oliveira, L. M. Ferreira, H. S. Martinho, and A. A. Martin, "FT-Raman spectroscopy for the differentiation between cutaneous melanoma and pigmented nevus," Acta Cir. Bras. **25**(4), 351–356 (2010).
51. P. A. Philipsen, L. Knudsen, M. Gniadecka, M. H. Ravnbak, and H. C. Wulf, "Diagnosis of malignant melanoma and basal cell carcinoma by in vivo NIR-FT Raman spectroscopy is independent of skin pigmentation," Photochem. Photobiol. Sci. **12**(5), 770–776 (2013).
52. T. J. Vickers, R. E. Wambles, Jr., and C. K. Mann, "Curve Fitting and Linearity: Data Processing in Raman Spectroscopy," Appl. Spectrosc. **55**(4), 389–393 (2001).
53. F. Knorr, Z. J. Smith, and S. Wachsmann-Hogiu, "Development of a time-gated system for Raman spectroscopy of biological samples," Opt. Express **18**(19), 20049–20058 (2010).
54. E. C. Le Ru, L. C. Schroeter, and P. G. Etchegoin, "Direct measurement of resonance Raman spectra and cross sections by a polarization difference technique," Anal. Chem. **84**(11), 5074–5079 (2012).
55. A. P. Shreve, N. J. Cherepy, and R. A. Mathies, "Effective Rejection of Fluorescence Interference in Raman Spectroscopy Using a Shifted Excitation Difference Technique," Appl. Spectrosc. **46**(4), 707–711 (1992).
56. K. Sowoidnich and H.-D. Kronfeldt, "Fluorescence Rejection by Shifted Excitation Raman Difference Spectroscopy at Multiple Wavelengths for the Investigation of Biological Samples," ISRN Spectroscopy. **2012**, 1–11 (2012).
57. B. Brozek-Pluska, J. Musial, R. Kordek, E. Bailo, T. Dieing, and H. Abramczyk, "Raman spectroscopy and imaging: applications in human breast cancer diagnosis," Analyst (Lond.) **137**(16), 3773–3780 (2012).
58. J. Zhao, M. M. Carrabba, and F. S. Allen, "Automated Fluorescence Rejection Using Shifted Excitation Raman Difference Spectroscopy," Appl. Spectrosc. **56**(7), 834–845 (2002).
59. A. A. M. Ana, P. de Oliveira, L. Silveira, Jr., R. A. Zangaro, and M. Zampieri, Proc. SPIE **5321**, 111 (2004), doi:10.1117/12.527793 Application of principal components analysis to diagnosis hamster oral carcinogenesis: Raman study.
60. G. J. Puppels, J. H. F. Olminkhof, G. M. J. Segers-Nolten, C. Otto, F. F. de Mul, and J. Greve, "Laser irradiation and Raman spectroscopy of single living cells and chromosomes: Sample degradation occurs with 514.5 nm but not with 660 nm laser light," Exp. Cell Res. **195**(2), 361–367 (1991).
61. I. Notingher, S. Verrier, H. Romanska, A. E. Bishop, J. M. Polak, and L. L. Hench, "In situ characterisation of living cells by Raman spectroscopy," Spectroscopy **16**(2), 43–51 (2002).

1. Introduction

Carcinomas in the area of the head and neck are among the fifth most common cancer diseases in men [1] with the majority originating from the mucosa [2]. Despite the oral accessibility, a majority of the lesions is diagnosed at a late stage of the disease, with more

#212874 - $15.00 USD Received 26 May 2014; revised 16 Jul 2014; accepted 31 Jul 2014; published 28 Aug 2014

than 60% of the patients suffering from a tumor in stage T3 or T4 at the time of diagnosis [1, 3, 4]. This implies a significant effect on the comparably poor five-year survival rate of 40%, as stated by the world health organization [5]. Despite the progress in surgery and radio-chemotherapy, no significant improvements regarding patient survival could be observed in the last decades [5]. It has been shown that the survival rate correlates highly with the stage of the disease [6]. The delayed recognition is mainly attributed to insufficient methods of cancer screening and diagnosis [4, 7]. Thus, the need arises for adequate, highly specific and objective methods for early cancer diagnosis. The current "gold standard" in the diagnosis of oral cancer is the visual inspection followed by an invasive biopsy and histopathological examination of the suspicious specimen. This inherits a variety of limitations. Inter-individual expertise in physical examination as well as in histopathological confirmation, the demand for human and financial resources, the delay in time, amount of tissue gained via biopsy, and the obligatory invasiveness of a biopsy are factors affecting early diagnosis and thus adequate and early treatment of cancer [4, 8–11]. Furthermore, since the majority of oral squamous cell carcinomas develop from precursor lesions of varying malignant potentials such as leukoplakia and dysplasias, multiple biopsies often become necessary over time to monitor the precursor spots and identify the need for treatment at an early stage. This inevitably affects patient compliance in a negative way and thus hinders adequate monitoring.

Bio-optical methods could overcome these limitations by relying on a common principle: When illuminating the tissue with light, the optical spectrum derived from the tissue contains information about the molecular/chemical composition of the tissue and/or its surface character [12]. The acquired information thus allows for a characterization of the tissue. A number of bio-optical methods - recently presented in literature [13, 14] - show the trend towards an in situ identification of pathological changes in clinical practice. These prospects have also been studied in the area of head and neck cancer, where mainly fluorescence/diffuse reflectance spectroscopy, optical coherence tomography (OCT) and confocal microscopy are currently applied [15–18]. By applying diffuse reflectance and fluorescence spectroscopy, a specific spectrum can be obtained from the biological sample within a fast acquisition time, but deriving specific molecular information from these spectra is challenging. Besides, OCT and confocal microscopy are mainly considered to be "imaging" techniques by increasing the contrast for a better visual identification of the pathological changes on a macro-scale or by portraying the conditions of the pathological changes on a micro-scale. Thus, the need for a subjective interpretation through the clinician cannot be bypassed entirely. Furthermore, to provide more accurate results, the use of exogenous labels - systemically applied in case of OCT or directly applied in the oral cavity in case of fluorescence – is necessary. However, the use of labels is accompanied by clinical restrictions and inherits certain risks for the patient.

Raman spectroscopy on the other hand provides an objective, high-precision and sensitive acquisition of the molecular tissue composition through the specific interaction of photons with cellular molecules [12]. Not needing a preparation of the biological samples in the form of exogenous labels or stains make Raman spectroscopy a non-invasive and robust tool for in situ analysis of biological tissue [19]. Furthermore, the high spatial and spectral resolution – up to single molecule recognition - can provide an exact localization of the lesion and its borders [20]. Prior works demonstrated the feasibility of Raman Spectroscopy in medical diagnosis regarding the identification of different pathologies and their stage of disease as well as their differentiation from physiological forms [21]. Current advances in Raman spectroscopic instrumentation, data processing and statistical analysis have led to promising results regarding spectroscopic cancer diagnostics in tissue bulks and histological sections as well as in cyto-pathological samples. Additionally, the independency of labeling and staining has enabled the identification of circulating malignant cells in body fluids [22–26]. Raman studies in the field of cancer originating from epithelia are reported for a variety of anatomical sites including oesophagus, skin, the gastrointestinal system, breast tissue and the cervix [27–34]. Recent studies reveal the potential for an identification of different pathologies in the area of the head and neck through Raman spectroscopy [35–38]. The feasibility of Raman spectroscopy as a method for the identification of OSCCs and its

#212874 - $15.00 USD Received 26 May 2014; revised 16 Jul 2014; accepted 31 Jul 2014; published 28 Aug 2014

malignancy-related changes has been demonstrated in prior works [39, 40]. First *in vivo* studies showed that the discrimination between healthy, malignant and premalignant oral tissue lesions is achievable and even early dysplastic stages of oral malignancy may be differentiated sufficiently due to its high sensitivity regarding molecular changes in the tissue [41–43]. According to these preliminary *in vivo* findings, recent works on oral spectral cytopathology showed that malignant cells can be differentiated significantly from physiological oral cells, even if morphological criteria do not indicate cancerous alterations [24], whereas studies on oral cell lines evaluate the role of radio-therapeutic resistance by investigating their spectroscopic patterns [44]. The spectral changes are mainly assignable to the change of the concentration of nucleic acids relative to the concentration of proteins and will be discussed in more detail later [42, 43, 45, 46]. While the Raman spectra of healthy oral tissue show the characteristics of lipids, the Raman spectra of malignant tissue carry the characteristics of proteins. Regarding these advances in recent works, Raman spectroscopy can provide information that is complementary or even superior to conventional techniques in oral pathology [40]. However, the impairment of the Raman signal through tissue auto fluorescence signals still raises the question of the optimal method for an automated, rapid, effective luminescence background separation, which is urgently needed for broad clinical applications. Thus, in the present work, the feasibility of shifted-excitation Raman difference spectroscopy (SERDS) for differentiation of cancerous from healthy tissue in *ex vivo* oral squamous cell carcinoma identification is studied. The findings of this study provide evidence that the approach of spectral acquisition by SERDS yields reproducible and significantly different results in terms of molecular composition in benign and malignant oral tissue – in particular in regions of proteins and lipids.

2. Material and methods

Study patients

The *ex vivo* experiments were conducted on resected samples of oral squamous cell carcinoma. The samples were obtained from 12 patients. All patients have undergone a surgical excision of an OSCC in inpatient care. The cohort comprised OSCC samples from 12 patients (10 males / 2 females; age 60.9 + - 10.6 years) (Table 1). The T-stage for classification of the pathology was n = 3 for T1 classified tumors, n = 6 for T2 and n = 3 for T3 tumors of the oral cavity. The location of the tumors has been determined as follows: n = 9 on the floor of the mouth, n = 2 on the lower alveolar crest and n = 1 on the oral hard palate (Table 2). The tumor samples were excised with a safety margin of 1 cm of physiological oral mucosa. The samples were measured within a post-excision time of 3 hours at a room temperature of 22°C. Pre-preparation of the tissue samples consisted of careful manual rinsing with a sterile saline solution to clean them from superficial contamination and necrotic tissue remnants as well as blood clots. All experimental proceedings were conducted on the day of surgery with a maximum *ex vivo* time of three hours. Other than the oral malignancy, the patients did not suffer from local or systemic diseases that could affect the optical examination of the oral mucosa. The study protocol was approved by the Ethics Committee (Ref. no. Az. 243_12). All patients gave written informed consent for the study prior to surgery.

Table 1. Descriptive characteristics: patient cohort.

	Gender		Total
	Male	**Female**	
n	10	2	12
Age (years) mean + - SD	62.2 + –10.7	54.5 + - 10.6	60.9 + –10.6
min	40	47	40
max	77	62	77

#212874 - $15.00 USD Received 26 May 2014; revised 16 Jul 2014; accepted 31 Jul 2014; published 28 Aug 2014

Table 2. Descriptive characteristics: oral tissue samples.

Histogenesis		Oral Squamous Cell Carcinoma
Type		Primary Tumor
	T1	3
	T2	6
	T3	3
Localization		Oral Cavity
	Floor of the mouth	9
	Lower alveolar crest	2
	Oral hard palate	1
N	Total	12
Measurement points		72

Raman spectroscopy SERDS - setup

Figure 1 shows the setup of the Raman experiment used for the characterization of the tissue. A diode laser (Toptica DLpro) with a variable laser wavelength between 770 and 810 nm was used as the excitation light source. A Glan-laser prism transparent for s-polarized light in combination with a half-wave plate allowed for the attenuation of the laser output power of 1 W down to 115 mW (not shown in Fig. 1). The excitation beam is launched into a glass fiber, which guides the laser radiation to a cage system. A short pass filter (785 nm) purifies the laser radiation from interfering signals originating from fiber-light interactions. The excitation laser is expanded to approximately 50 mm and then reflected via a dichroic mirror - highly reflective for excitation wavelengths but transparent for red shifted wavelengths - through the focusing lens into the laser focus (diameter approximately 200 µm) being the probe volume. A portion of the excited signals is detected in back-scattering direction through the focusing lens. The shifted fluorescence and Raman signals pass the dichroic mirror and are launched via another focusing lens into a detection glass fiber bundle, guiding the signals to the spectrometer (QE 65000 from Ocean Optics) with a long-pass filter (785nm, Raman Razor Edge filter) suppressing the elastically scattered light that passes the dichroic mirror. For an efficient detection of the signals, the spectrometer is operated without an entrance slit. Instead, the linear arrangement of the 100 µm core diameter single fibers within the fiber bundle serves as the slit. At the interface of the fiber bundle not connected to the spectrometer, the single fibers are arranged in a round pattern - enabling the efficient coupling of the signals into the fiber bundle. During the SERDS measurements, spectra are first acquired when the excitation wavelength is set to *1 (783nm, see below). Then the excitation wavelength is shifted slightly to *2 (785nm), where the second spectral data set is acquired. The spectra corresponding to each excitation wavelength are averaged and then the mean spectrum corresponding to *1 is subtracted from the mean spectrum corresponding to *2.

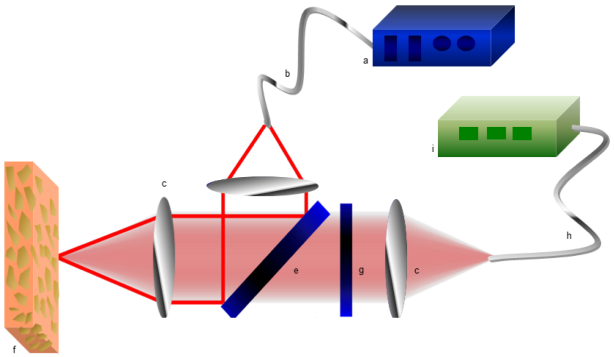

Fig. 1. Raman spectroscopic setup a) excitation diode laser (variable wavelength), b) excitation glass fiber, c) lens, d) lens f = 100 mm, e) dichroic beam splitter 800nm, f) biological tissue, g) long pass filter 785 nm, h) detection glass fiber bundle, i) spectrometer.

#212874 - $15.00 USD Received 26 May 2014; revised 16 Jul 2014; accepted 31 Jul 2014; published 28 Aug 2014

Measurement procedure

During optical measurements, the samples were put on a matte black paper. In order to avoid overlapping of the measuring points, a minimum standardized distance of 5 mm was maintained between the measurement points. For each tissue sample, six measurement points were visually determined. Three measurement points were defined as visually classified physiological mucosa in the marginal area of the resected tissue. Three measurement points in the parts of the tissue classified as OSCC. The visual selection of the measurement points was confirmed by the responsible surgeon of the Department of Oral and Maxillofacial Surgery. Seventy-two measurements were made in total per wavelength, covering 12 samples of oral mucosa, each analyzed at three physiological and three pathological tissue points (12 x 6 = 72). The optical measurements were conducted with a standardized distance of 10 cm under a vertical alignment of the probe/excitation light to the tissue sample. The diameter of the excitation light spot can be estimated to be smaller than 0.2 mm on the tissue. The measurements were conducted under residual stray light, to mimic the parameters of in situ measurements in the oral region on the patient. After each measurement, the point of measurement was marked with a colored needle that depicted the point as OSCC or physiological mucosa (red: OSCC; blue: physiological). After measurement proceedings, the resected tumor tissues were processed at the Institute for Pathology, University Hospital Erlangen, Germany, as part of the conventional histopathological routine evaluation as well as for a histological confirmation of each measurement point as seen in Fig. 2.

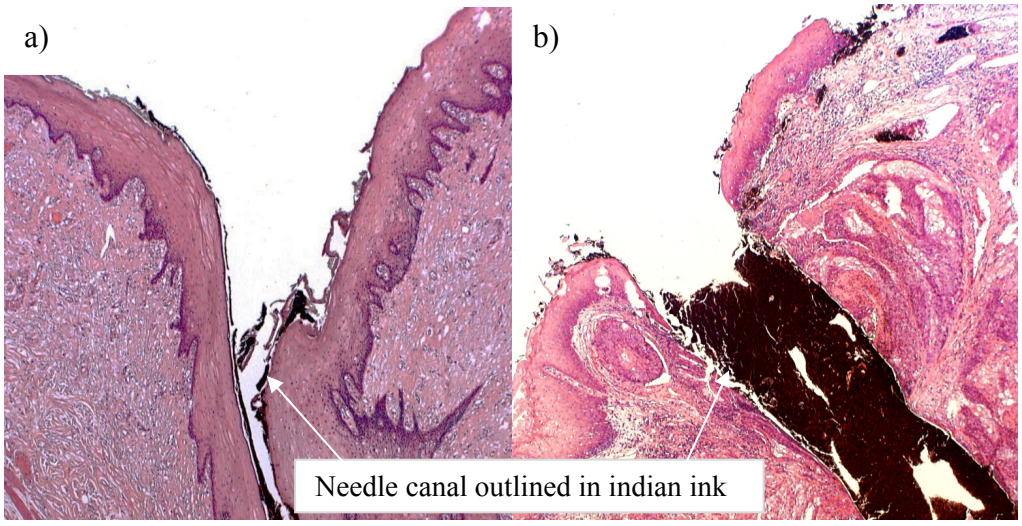

Fig. 2. Histological confirmation of each measurement point (2,5x magnification / haematoxylin eosin stained slide) a) physiological tissue b) pathological OSCC lesion.

Spectral data acquisition and processing

For each point of measurement (6 measurement locations on each of the 12 mucosa samples), 50 single spectra were acquired for each of the two excitation wavelengths. The signal integration time of one spectrum was set to 3 s. Therefore the acquisition of 50 spectra took 150 s. The excitation wavelength can be varied reproducibly in the computer menu interface of the laser. The wavelength can be varied from 783 to 785 nm within few seconds. As excitation wavelengths we chose 783 and 785 nm, since the SERDS technique provided the best differentiability between benign and malign tissue for this width. As shown in Fig. 3, the Raman spectrum of the tissue is purified from interfering fluorescence emissions: In a first step, a mean spectrum is computed from the 50 single spectra separately taken from one

#212874 - $15.00 USD Received 26 May 2014; revised 16 Jul 2014; accepted 31 Jul 2014; published 28 Aug 2014

measurement location for each of the two excitation wavelengths. Since we used the wavenumber range from 1000 to 1800 cm-1 for the statistical analysis of the SERDS spectra [45], the area of the two mean spectra in this wavenumber range was normalized in a second step. Subsequently, in a third step, the two remaining intensity-normalized mean spectra were subtracted to eliminate the fluorescence background according to the SERDS technique. Subsequently in a third step, the two remaining intensity-normalized mean spectra were subtracted to eliminate the fluorescence background according to the SERDS technique. In a following fourth step, we reconstruct the Raman spectrum which after reconstruction is not on the zero-baseline. In a fifth step, a Savitzky Golay filter (polynomials of order 5) is applied to the reconstructed "Raman spectrum" and the fitted function is then in a sixth step subtracted from the reconstructed Raman spectrum. As a consequence the broadband background is removed from the reconstructed Raman spectrum as it can be seen for the pathological and physiological tissue at the very bottom in Fig. 3.

#212874 - $15.00 USD Received 26 May 2014; revised 16 Jul 2014; accepted 31 Jul 2014; published 28 Aug 2014

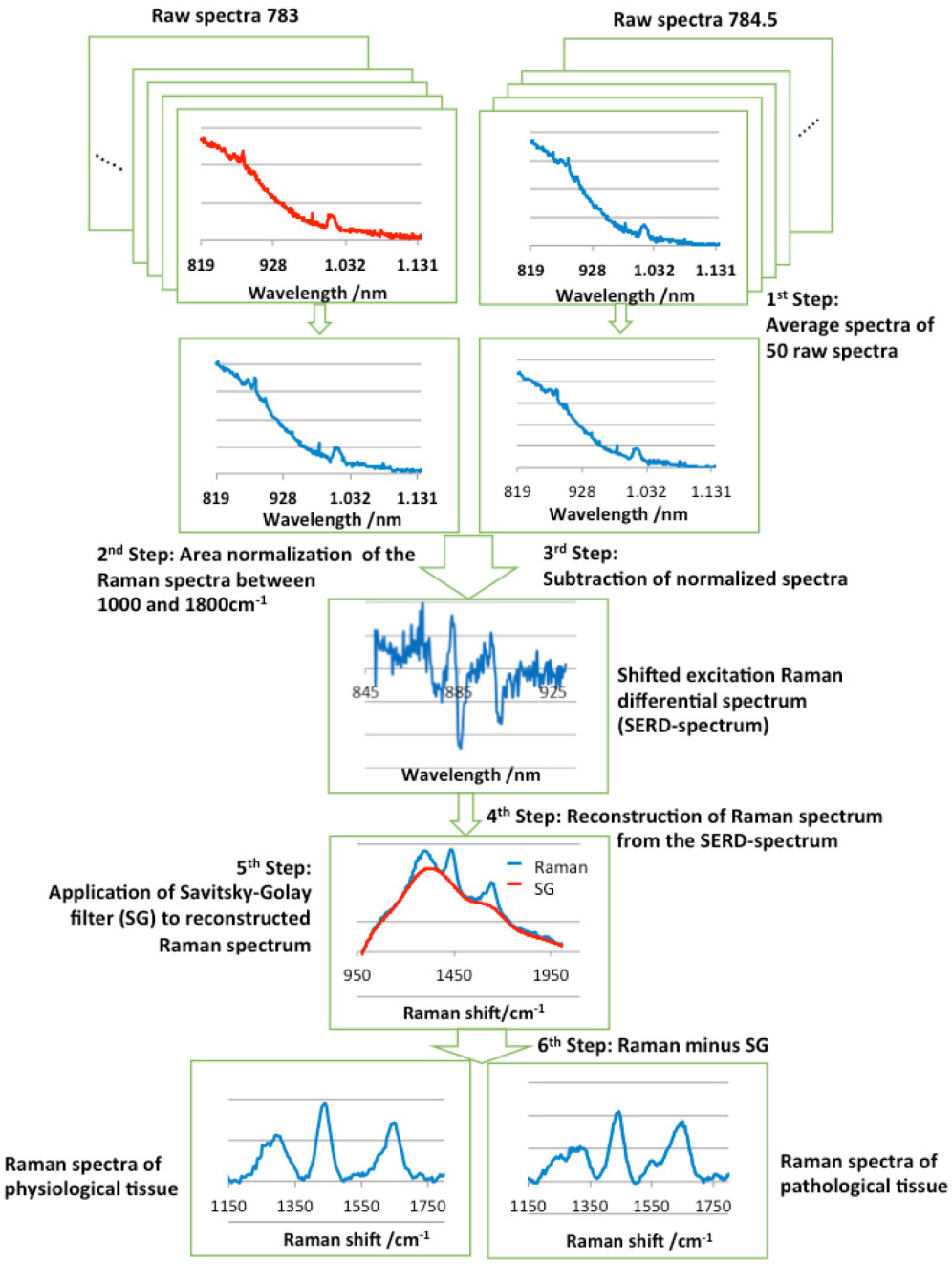

Fig. 3. Spectra processing procedure.

Statistics

To discriminate between healthy and tumor tissue using the Raman fingerprint signal, we utilized a linear discriminant analysis (LDA) [47]. An LDA estimates the statistical distribution of the classes healthy and tumor assuming two normal distributions. Hence, a previously unseen observation can be assigned to one of the classes based on this estimation. As the classification performance of LDA is hampered by high dimensionality of the data, we

#212874 - $15.00 USD Received 26 May 2014; revised 16 Jul 2014; accepted 31 Jul 2014; published 28 Aug 2014

performed a dimensionality reduction of the data set based on principal component analysis (PCA) [47]. PCA produces a transformation of the original data set with following characteristics: the transformed variables (principal components – PCs) are linear combinations of the original variables, with the property that the order of the PCs represents the amount of variability in the data explained by the PCs. This means, the first PC explains the largest part of the variability, the second PC the second largest and so on. As we can assume that we do not need to explain 100% of the variability to be able to perform discrimination between the classes of interest, we can reduce the number of variables by using only a limited number of PCs.

The classification performance of this combination of PCA and LDA was calculated by a cross-validation. The data set was divided into twelve parts, each part consisting of the measurements of one patient. In a loop consisting of twelve iterations, eleven of the twelve parts were used to perform the PCA and the LDA. For the twelfth part, the probability to belong to the class tumor or healthy tissue was predicted using the previously trained PCA and LDA. In each cross-validation step, the optimal number of PCs to discriminate between healthy and tumor tissue was estimated by nested cross-validation. After calculating twelve steps, the probabilities for all observations in the data set were estimated. Subsequently, the classification error was calculated by comparing the predicted tissue with the actual tissue. ROC analysis provided sensitivities and specificities for all possible cutpoints to determine tissue type with tissue probabilities. All calculations were performed using the statistical software package R V3.1.0 [48].

Results

In the eleven cross-validation loops, 40 principal components were selected 6 times, 45 PCs were selected 3 times, 55 PCs were selected twice and 50 PCs were selected once. The mean percentage of variation explained by the first four PCs in the 12 cross-validation runs were 76.2%, 10.7%, 5.8%, and 2.4%. Of the 72 observations, 34 were correctly classified as healthy, and 31 were correctly classified as tumor tissue. Five tumor measurements were falsely classified as healthy and two normal tissue measurements were falsely labeled as tumor tissue. This means that the classification error estimated by the cross-validation was 9.7% with a sensitivity of 86.1% and a specificity of 94.4%. Discrimination accuracy between tumor tissue and physiological tissue was measured with an AUC of 94.5% (Fig. 4). Figures for mean Raman spectra for OSCC and physiological tissue are shown in Fig. 3.

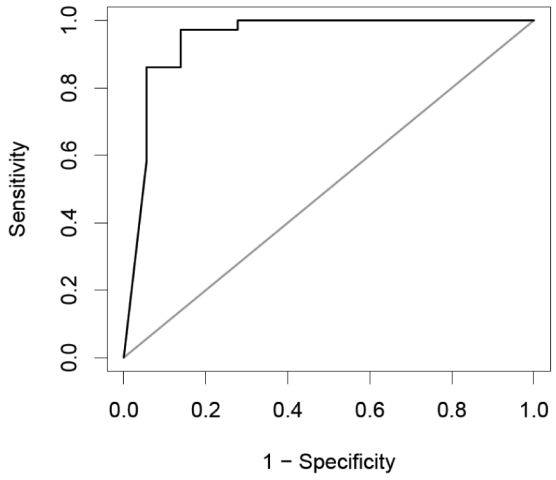

Fig. 4. Receiver operating characteristic (ROC) curve representing the diagnostic accuracy with an area under the curve (AUC) of 0.945.

#212874 - $15.00 USD Received 26 May 2014; revised 16 Jul 2014; accepted 31 Jul 2014; published 28 Aug 2014

The differentiability of malign and benign tissue from the oral cavity can be attributed to spectral features of lipids and proteins in the Raman shift range between approximately 1000 and 1800 cm-1. Figure 5 shows exemplary Raman spectra of pathological and physiological oral tissue and assigns the Raman signal peaks to molecular vibrations. The assignment to molecular vibrations was taken over from Venkatakrishna et al. [45] and Oliveira et al. [46].

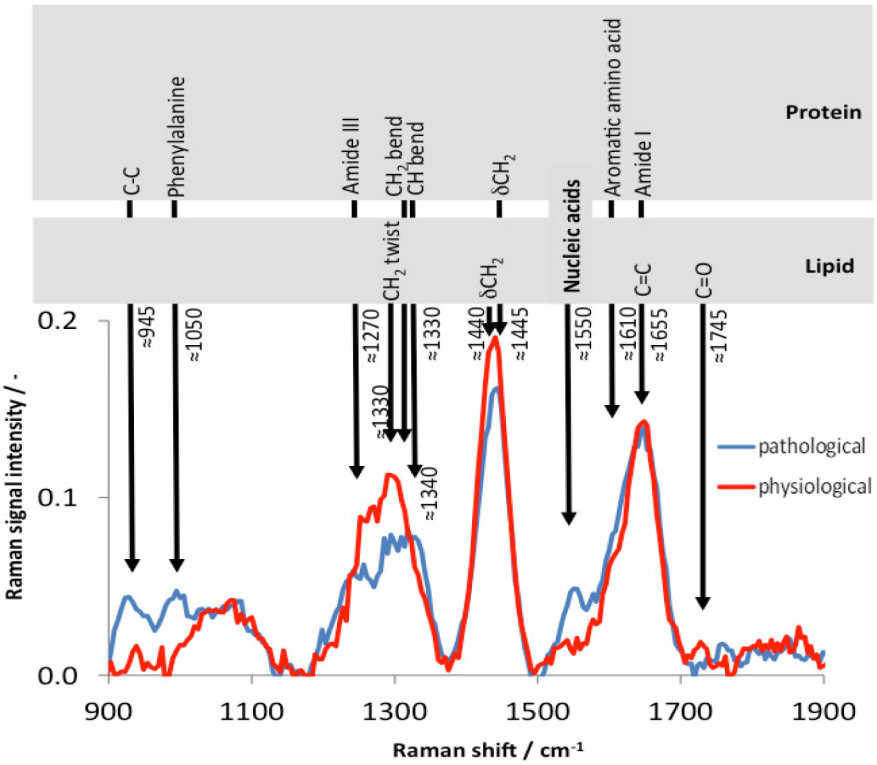

Fig. 5. Assigment of spectral features of proteins, lipids and nucleic acids to the ones of pathological and physiological oral tissue.

Discussion

A significant challenge for Raman spectroscopy in biomedical applications is the removal of concomitant background fluorescence without the loss of relevant and significant Raman spectral features which account for the biomolecular profile of the tissue. The acquired raw spectrum contains a weak Raman signature compared to the intense fluorescence background (fluorescence orders of magnitude more intense than Raman scattering). This interference limits the applicability of Raman spectroscopy in the clinical environment [49]. This immensely hinders the performance of cancer identification. Recent efforts have been made to remove the underlying fluorescence background from the spectral data in an effective manner and adequate Raman instrumental systems or data processing regimes have been introduced. Computational approaches primarily focus on the polynomial fit method or Fourier transformation of the acquired data [50–52], whereas time-resolved Raman spectroscopy and polarization modulation have been described in literature regarding instrumental approaches [53, 54].

A further possible instrumental approach - as applied in this study - is the Shifted Excitation Raman Differential Spectroscopy (SERDS) [55]. This approach – primarily described in 1992 by Mathies et. al - exploits the fact that the Raman spectrum shifts according to small shifts of the excitation photon energy (excitation wavelength), while the

#212874 - $15.00 USD Received 26 May 2014; revised 16 Jul 2014; accepted 31 Jul 2014; published 28 Aug 2014

fluorescence spectrum remains unaffected by small shifts of the excitation photon energy [55]. Through a slight shift in the excitation wavelength, two different spectra are acquired, both containing the background fluorescence spectrum and the desired Raman spectrum. Through the subsequent subtraction of the two acquired spectra, the background fluorescence spectrum can be removed. Prior findings suggest the feasibility of SERDS as a reproducible, precise and systematic approach for luminescence suppression in the biological tissues flesh, fat, connective tissue, and bones [49, 56]. The results of our study suggest a high identification of OSCC lesions with a sensitivity of 86.1%. An even higher identification of physiological tissue can be observed (94.4%). This is crucial for a diagnostic test as it does not produce unnecessary false positive results. For a better comparison of the diagnostic method, the area under the ROC curve (AUC) was calculated (see Fig. 4). With a value of 95.4%, the calculation yielded a result that can be interpreted in the range of an excellent diagnostic test.

The data presented in this work demonstrates that Raman spectra acquired with the SERDS technique are reproducible and sensitive to nucleic acids, lipids and proteins (Fig. 5). A comparison of the acquired spectra to prior works in this field shows a high correlation of these spectral features to the spectral data acquired with the SERDS method: While spectral features assignable to lipids, such as the C = O vibration at 1745 cm-1, the δCH2 vibration at 1440 cm −1 or the CH2 twist vibration at 1330 cm-1 are clearly less pronounced in the pathological tissue, other spectral features assignable to proteins are clearly more emphasized in the pathological tissue. Singh et al. [41] give two explanations for the protein dominance in the pathological tissue. Firstly there is a loss of architectural arrangement of different layers in the pathological tissue. Therefore the lipid characteristics are reduced if the content of different layers is mixed. Secondly the number of surface and receptor proteins, antigens, antibodies and enzymes is high in cells of pathological tissue, which is assumed to give rise to protein dominated spectra [42]. These results are also in concordance with other cancerous tissues such as breast tissue, where the lipid profile of the tissue is seen as a Raman-biomarker for a distinction of benignant and malignant breast tissue [32, 57]. The spectral feature of nucleic acids at 1550 on the other hand is emphasized in OSCC tissue. This spectral feature has also been observed in prior studies and can be interpreted with regard to a higher concentration of nucleic acids in cancer tissue [46]. As this work could demonstrate the validity of SERDS in OSCC tissue, further studies can be carried out in a larger sample size to identify the specific biochemical composition and investigate spectral features that are altered in malignant oral tissue and its early malignant transformation. Recent developments in this field show great prospects for Raman spectroscopy to detect discrete molecular changes as an unsupervised method in bulk tissue as well as in cytopathological samples [24, 42].

Applying the SERDS method in clinical practice may come with several advantages. Firstly, the acquired SERDS spectra are meant to contain more information than computational methods [58]. When it comes to the highly sensitive differentiation of precancerous lesions and the monitoring of lesions with a high risk for degeneration, this might be an important benefit. Secondly, the acquired reference spectra do not come with “fixed pattern noise” originating from the setup or surrounding stray light when applying the SERDS method [55, 58]. Subsequently, a rather standardized database of reference spectra can be attained without influencing parameters of the setup or the clinical environment, for a more effective and accurate transfer of the findings to clinical practice. Thus, a Raman signal without interfering noise arising from varying stray light or the endoscopic setup can be acquired and a standardized data set can be obtained for lesions in the oral cavity. Since little or no standardization can be realized in clinical environments regarding the setup, angular distribution, distance to the sample and stray light, this feature might be a substantial benefit.

Prior Raman studies concerning oral squamous cell carcinomas suggested that the acquired spectral data can be linked to mathematical algorithms for an automatic objective classification of the suspicious region without the need for a subjective interpretation [59]. Accordingly, the data analysis used in this study is based on the conversion of the Raman

#212874 - $15.00 USD Received 26 May 2014; revised 16 Jul 2014; accepted 31 Jul 2014; published 28 Aug 2014

signal into a diagnosis through a supervised statistical learning procedure (LDA). This way, an objective classification into tumor tissue or physiological oral tissue can be derived from the acquired spectra, without the need for a subjective clinical interpretation of the results. For identifying the data that accounts for the differentiation, the spectral data was reduced to a new set of calculated variables, accounting for the majority of the data variance. Based on that, a classification model was established. This way, an effective and fast calculation performance can be yielded when transferring the system to *in vivo* clinical trials. The database we used in this study was derived from 12 tumor samples with 72 data points. This is a rather limited data set. However, the statistical analysis of the acquired Raman spectra shows sufficient and promising results that led to the establishment of an accurate classification model for OSCCs. Further studies have to be conducted to extend the database for an even more accurate classification and to validate the classification performance through independent data sets.

Even if a better performance could be achieved when setting the excitation wavelength in area range within 400-700nm, there are two main reasons for exciting the Raman scattering in the near infrared-region of 783 nm – 785 nm. First, biological tissue inherits a minimal absorption coefficient in the near-infrared region due to the low number of chromophores that are excitable at longer wavelengths. This feature substantially reduces the accompanied autoluminescence and accounts for a moderate autofluorescence contribution to the spectra [19, 58]. Second, excitation light in the near-infrared region prevents biological tissue from iatrogenic damage due to unwanted light-tissue interactions through water absorption like heating, coagulation and subsequent tissue necrosis.

The incident power was set to 115mW laser power at 783 nm. Since the laser power as well as the excitation wavelength highly correlates with the probability of tissue damage but also with the quality of the acquired Raman spectra, it is of major importance to set an excitation wavelength that addresses both needs in an adequate manner. Literature suggests a power incidence of over 80mW for an optimal signal-to-noise ratio, however the value is dependent on the investigated biological sample [49]. No significant affection of cells and their components was observed at 115mW laser power at 785nm in literature [19, 60, 61]. This is in accordance to our clinical findings after our spectral measurements, where no iatrogenic damage through the laser excitation light could be observed.

The wavelength shift performing the SERDS method was set to 2 nm. Higher $\Delta\lambda$ make a re-development of the Raman spectrum from the SERDS spectrum unemployable, while too little $\Delta\lambda$ would lead a low signal-to-noise ratio [58]. Literature suggests an optimal wavelength shift of 0.5nm when performing measurements on biological samples, however, the $\Delta\lambda$ is specifically dependent on the widths of the Raman peaks [49]. Thus we pre-examined the optimal wavelength shift for a first feasibility analysis. The best results could be obtained in our study sample with a shift of 2 nm. Even though very promising results could be obtained when performing the acquisition with $\Delta\lambda$ the chosen parameter set, further studies have to be conducted to find the optimal wavelength shift for the identification of oral cancer before conducting research on premalignant lesions (precursors) of OSCC and the transfer of the method to *in vivo* clinical trials.

Conclusion

Shifted Excitation Raman Differential spectroscopy (SERDS) was evaluated in terms of an *ex vivo* identification of oral squamous cell carcinoma with promising results for a non-invasive optical biopsy system. The method has proven to objectively identify OSCC tissue with excellent results and is capable of an adequate and valid extraction of the underlying Raman signal. The spectral features of proteins, lipids and nucleic acids can serve as sensitive Raman biomarkers to distinguish between cancerous and noncancerous oral tissue. The SERDS Setup as described in this study has a prospect to complement the standard approach of histopathological diagnosis.

Conflict of interest There was no conflict of interest.

#212874 - $15.00 USD Received 26 May 2014; revised 16 Jul 2014; accepted 31 Jul 2014; published 28 Aug 2014

Ethical approval This work was approved by the ethics committee of the University of Erlangen-Nuremberg (Ref. no. Az. 243_12).

Acknowledgment

This research work was supported by the Interdisciplinary Center for Clinical Research (IZKF) of the Clinical Center Erlangen; Krankenhausstr. 12, 91054 Erlangen, Germany. The present work was performed in fulfillment of the requirements for obtaining the degree "Dr. med." The authors gratefully acknowledge funding of the Erlangen Graduate School in Advanced Optical Technologies (SAOT) by the German Research Foundation (DFG) in the framework of the German excellence initiative. We acknowledge support by Deutsche Forschungsgemeinschaft and Friedrich-Alexander-Universität Erlangen-Nürnberg within the funding programme Open Access Publishing.

#212874 - $15.00 USD Received 26 May 2014; revised 16 Jul 2014; accepted 31 Jul 2014; published 28 Aug 2014